8A.2 PROCESS-ORIENTED DIAGNOSTICS FOR TROPICAL CYCLONES AND DISTURBANCES IN CLIMATE MODELS USING THE COLUMN-INTEGRATED MOIST STATIC ENERGY VARIANCE BUDGET

Jarrett C. Starr*, Allison A. Wing, Suzana J. Camargo, Daehyun Kim, Tsung-Yung Lee, and Jihong Moon
Florida State University, Tallahassee, Florida

1. INTRODUCTION

Tropical Cyclones (TCs) are represented in our general circulation models (GCMs), however longstanding biases exist in their ability to simulate TC frequency and intensity (Camargo and Wing, 2015). Process-oriented diagnostics (PODs) can be used to evaluate physical processes associated with meteorological phenomena in a model or suite of models in comparison to an observational reference, in order to identify targets for model improvement (Maloney et al., 2019; Neelin et al., 2023). The column-integrated moist static energy (MSE) spatial variance budget was used as a POD in Wing et al. (2019) to evaluate the three diabatic feedbacks of the budget in the TC intensification process across a suite of high resolution GCMs. This framework was then utilized in Dirkes et al. (2023) to evaluate 5 different reanalysis datasets in the same fashion.

The work in this study builds upon prior work using the MSE variance budget by comparing the GCMs in Wing et al. (2019), as well as many more high resolution GCMs, against each other and to the reanalyses in Dirkes et al. (2023). The representation of these feedbacks across the GCMs will also be compared against each other by grouping them by similar horizontal grid spacing, whether they are fully coupled versus uncoupled with the ocean, and investigating the effect of clouds. To more effectively compare the GCMs to a more "pure" observational reference rather than reanalyses, *CloudSat* satellite observations from Lee and Wing (2024) are utilized for the radiative feedbacks in the investigation of the role of clouds. This study also investigates the differences in feedback representation in ERA-5 precursor tropical disturbances that do or do not develop into TCs.

2. DATA AND METHODS

Five reanalyses are used in this study from Dirkes et al. (2023) as well as the six high resolution GCMs in Wing et al. (2019). There are also thirteen more high resolution GCMs that were analyzed. Of the nineteen GCMs that were used in this study, there were a vast range of horizontal grid spacings among them where some had ¼ of a degree grid spacing to as coarse as nearly 1.5-degree grid spacing.

**Corresponding author information: Jarrett C. Starr, Department of Earth, Ocean, and Atmospheric Science, Florida State University, 1011 Academic Way, Tallahassee, FL 32306; Email: jcs18e@fsu.edu*

Three of these models also had both a simulation that was fully coupled to the ocean and a simulation that was uncoupled and had prescribed sea surface temperatures (SSTs). All of the GCMs and reanalyses also had varying cloud, radiative, and convective schemes as well as different dynamical cores. The *CloudSat* satellite observations were radial profiles of the intensity bin composite feedbacks provided by Lee and Wing (2024). However, to more fairly compare the reanalyses and GCMs to these observations, the radial profiles were coarsened to 24 km.

Following Wing et al. (2019) and Dirkes et al. (2023), the MSE variance budget feedbacks are calculated in a 10-degree by 10-degree box domain centered on the TC at each time up until lifetime maximum intensity (LMI) for the GCMs and reanalyses. The azimuthal mean of each of these box snapshot feedbacks and the box-averaged feedback is calculated. Each of these snapshots are then binned and composited by the snapshot's maximum velocity (V_{max}) as well as minimum mean sea level pressure (minimum MSLP). The MSE variance budget and the feedbacks investigated in this study are provided in Figure 1. Considering Dirkes et al. (2023) noted one specific reanalysis dataset could not be deemed "better" than the others, we treat the reanalyses as a range of "observational" truth.

$$\frac{1}{2}\frac{\partial \hat{h}'^2}{\partial t} = \underbrace{\boxed{\hat{h}'F_k'}}_{h'SEF'} + \underbrace{\boxed{\hat{h}'N_L'}}_{h'LW'} + \underbrace{\boxed{\hat{h}'N_S'}}_{h'SW'} - \cancel{\hat{h}'(u\cdot\nabla h)'}$$

Figure 1: ***The MSE spatial variance budget and the diabatic feedbacks analyzed on the right hand side (boxed). The h'SEF' feedback is the surface enthalpy flux (SEF) feedback, h'LW' is the longwave (LW) feedback, and h'SW' the shortwave (SW) feedback.***

3. ROLE OF RESOLUTION

The GCMs were separated into different groupings based on their horizontal grid spacing to investigate their representation of the feedbacks compared to GCMs of similar and differing grid spacing. When observing the box-averaged feedbacks in Figure 2, we can note the differences in feedback representation of these GCMs with intensity. First comparing the top two rows, the ordering and magnitudes of the variance as well as the feedbacks is minimally different when binning by V_{max} versus minimum MSLP, therefore we stick with V_{max} to be consistent with prior work. The more finely gridded GCMs in the middle row tend to follow the reanalysis mean closely across the feedbacks and variance. The more coarsely gridded GCMs in the bottom two rows tend to be more variable and closer to the extremities of the reanalysis range. The SEF and SW feedbacks tend to be higher in the more finely gridded GCMs than the more coarsely gridded ones. The LW feedback is positive across all the GCMs and reanalyses but varies in magnitude.

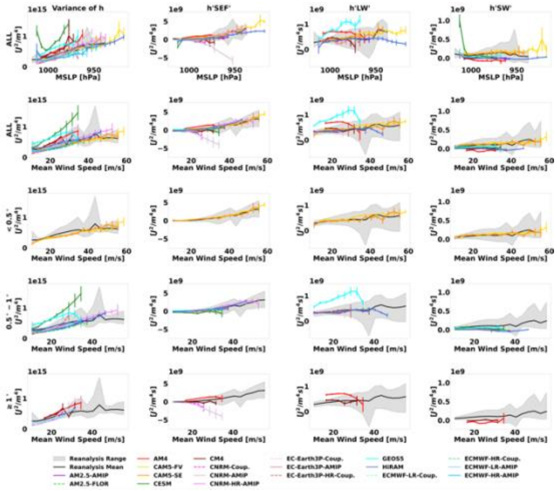

Figure 2: ***Box-averaged MSE variance and its feedbacks (columns) as a function of intensity (min. MSLP top, V_{max} bottom 4 rows), split by horizontal resolution (last 3 rows).***

4. ROLE OF COUPLING

For the three models with fully coupled and uncoupled simulations, the azimuthal mean SEF feedback was higher in the uncoupled simulation than the coupled simulation across all intensity bins (top row of Figure 3). To understand why this difference was present, the SEF feedback was decomposed.

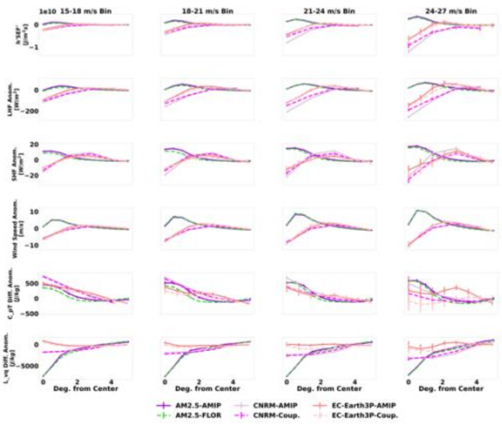

Figure 3: ***Azimuthally averaged SEF feedback and its components (rows) by intensity (columns) in coupled and uncoupled model simulations.***

First observing the latent and sensible heat flux anomalies (second and third row of Figure 3, respectively), where these anomalies peaked radially, they were higher in the uncoupled simulations as well. Assuming the SEFs were calculated using a bulk equation, the wind speed and air-sea enthalpy disequilibrium anomalies are of importance as well. Ultimately, the wind speed anomalies did not exhibit meaningful differences between the simulations (fourth row of Figure 3). However, the anomaly of the thermal component of air-sea enthalpy disequilibrium does indicate the uncoupled simulations have higher anomalies in the TC-core region (innermost 2.5 degrees). Minimal differences exist between the coupled and uncoupled representation of the anomalies of the moisture component of air-sea enthalpy disequilibrium.

5. ROLE OF CLOUDS

The feedbacks presented in this section are calculated a bit differently compared to the way they are described in the methodology to match that of *CloudSat*. Instead of the feedbacks being calculated at each snapshot, they are now calculated from the intensity bin composite MSE and flux. The SW feedback also now does not include the zero values of SW flux convergence at night to match that of what is used in the *CloudSat* calculations.

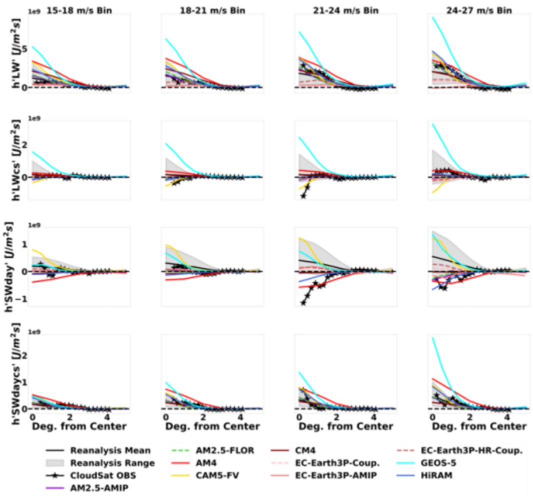

Figure 4: ***As in Fig. 3, but with just the total and clear-sky radiative feedbacks for GCMs with the necessary output, reanalyses, and CloudSat.***

The azimuthal mean radiative feedbacks (total and clear-sky) are depicted in Figure 4. At weaker intensities, the GCMs and reanalyses tend to have a higher total LW feedback in the TC-core region compared to *CloudSat*, but at stronger intensities the GCMs and reanalyses fall more closely to observations. The clear-sky LW feedback tends to be near zero at all intensities across the GCMs, reanalyses, and *CloudSat*. The total SW feedback in the GCMs is near zero at weaker intensities, but diverges at higher intensities where some have a positive or negative feedback. The *CloudSat* total SW feedback is also near zero at weaker intensities, but becomes more negative in the TC-core at higher intensities. The clear-sky SW feedback is slightly positive in the TC-core region at all intensities across the GCMs, reanalyses, and *CloudSat*.

6. TROPICAL DISTURBANCES

Precursor tropical disturbances that may or may not end up developing into TCs were investigated in ERA-5 over the years of 2000-2004 using the same MSE variance budget used on the TCs. These disturbances were given a tag variable that indicated if they reached TC status. The disturbances that did develop and their corresponding snapshots were binned and composited together by intensity and compared to the binned and composited snapshots of disturbances that did not develop.

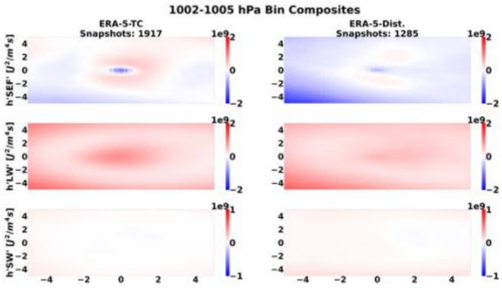

Figure 5: ***Spatial view of MSE variance budget feedbacks (rows) for developing and non-developing disturbances (columns) in ERA-5 binned by min. MSLP.***

The developing disturbance intensity bin composite SEF feedback shows a more closed ring of positive feedback. While the LW feedback is positive in both cases, the developing disturbances have a much more circular pattern in the TC-core region and is more strongly positive than the non-developers. The SW feedback is just slightly more positive in the non-developers than that of the developers. This would be anticipated however as ERA-5 was the only reanalysis of the five investigated to have a negative SW feedback for the TC intensity bin composites. Therefore, as the developers reach stronger intensities the SW feedback decreases.

References

Camargo S.J., and A. A. Wing, 2015: Tropical cyclones in climate models. *WIREs Climate Change*, **7 (2)**, 211–237.

Dirkes, C. A., A. A. Wing, S. J. Camargo, and D. Kim, 2023: Process-oriented diagnosis of tropical cyclones in reanalyses using a moist static energy variance budget. *Journal of Climate*, **36 (16)**, 5293–5317

Lee, T.-Y., and A. A. Wing, 2024: Satellite-based estimation of the role of cloud-radiative interaction in accelerating tropical cyclone development., in revision.

Maloney, E. D., and Coauthors, 2019: Process-oriented evaluation of climate and weather forecasting models. *Bulletin of the American Meteorological Society*, **100 (9)**, 1665–1686.

Neelin, J. D., and Coauthors, 2023: process-oriented diagnostics: Principles, practice, community development, and common standards. *Bulletin of the American Meteorological Society*, **104 (8)**, E142–E1468.

Wing, A. A., and Coauthors, 2019: Moist static energy budget analysis of tropical cyclone intensification in high-resolution climate models. *Journal of Climate*, **32 (18)**, 6071–6095.